

Impurity effects and bandgap-closing in massive Dirac systems

Habib Rostami¹ and Emmanuele Cappelluti^{2,3}

¹*Istituto Italiano di Tecnologia, Graphene Labs, Via Morego 30, I-16163 Genova, Italy*

²*Istituto dei Sistemi Complessi, CNR, 00185 Roma, Italy*

³*Dipartimento di Fisica, Università La Sapienza, P.le A. Moro 2, 00185 Roma, Italy*

(Dated: May 3, 2018)

We investigate the effects in the spectral properties of a massive Dirac system of the dynamical renormalization induce by disorder/impurity scattering within the self-consistent Born approximation. We show how that these effects leads to a remarkable closing of the bandgap edge. Above a critical value U_c of the impurity scattering the gap eventually closes, giving rise a finite density of states at zero energy. We show that the bandgap closing stems from the quasi-particle dynamical renormalization and it is not associated with the vanishing of the effective massive term. Incoherent processes are fundamental to describe such physics.

I. INTRODUCTION

Low dimensional electronic properties of graphene are commonly described by the Dirac model, resulting in two Dirac cones with linear dispersion[1]. Controlling and tailoring the properties of such dispersion, in particular in regards with the possibility of opening a gap, is one of the most important challenges in the field, from the theoretical as well as technological point of view. The most straightforward way of opening a gap in graphene is by explicitly inducing a breaking of the sublattice symmetry,[2–6] as for instance obtained in graphene/SiC, [4] hexagonal Boron Nitride (h-BN),[7, 8] graphene/h-BN,[9–11] and graphene/h-BN superlattices.[11–13] Similar physics is obtained, with a mapping pseudospin \rightarrow real spin, in the surface state of 3D topological insulator in the presence of a Zeeman field.[14–16] In all these examples the breaking of symmetry is reflected in the appearance of a *massive* term $\propto \Delta \hat{\sigma}_z$ in the Dirac model, where the Δ represents the energy difference in the two sublattices, mapped in the two components of the Dirac spinor. The same paradigmatic massive Dirac model is also ofte used to describe single-layer transition metal dichalcogenides,[17] after neglecting the momentum dependence of the mass term. [18] Other possible single-particle sources of bandgap can come be the Haldane mass $\propto \Delta \tau_z \hat{\sigma}_z$ [19] and the intrinsic spin-orbit coupling $\propto \Delta s_z \tau_z \hat{\sigma}_z$ [20] with $\tau_z = \pm$ and $s_z = \pm$ as the valley and spin degree of freedoms, respectively.

Many-body effects (e.g electron-electron and electron-phonon interaction, impurity scattering etc.) are also crucially relevant in graphene, giving rise to a variety of interesting phenomena as a the minimum conductivity at zero bias [21], marginal Fermi liquid [22, 23], the linear dependence of conductivity with doping [21], plasmaronic effects in the band dispersions [24] and so on. From a general point of view, however, the presence of the (spinless) massless nature Dirac cones in the graphene is protected against any single-particle and many-body perturbations, at least as long as the interaction does not lead to a spontaneous breaking of symmetry, usually above a finite critical coupling strength.[25–41]

Among the possible sources of interaction, disorder/impurity scattering represents the most direct and simple case, provided a conserving approach is enforced. Impurity/disorder effects have been hence thoughtfully analyzed in graphene and in the massless Dirac model. [42–46] Relatively less attention has been devoted to the study of disorder effects in the *massive* Dirac model. However, in spite of the simplicity, the analysis of impurity effects in the massive Dirac mode gives rise to interesting novel features. For instance, the possibility of a bandgap closing above a threshold of impurity scattering, was briefly mentioned in Ref. [47], in the simplest paradigmatic context of a self-consistent Born approximation (SCBA), but a careful characterization of such bandgap closing and of its origin has not been provided. Note that such scenario (observed in the simple SCBA scheme) is qualitatively different from the onset of midgap states in highly disordered massive Dirac models,[48–51] which needs a *t*-matrix approach to be revealed and that can be more correctly interpreted as *gap filling* rather than *gap closing*.

In this paper we present a detailed analysis of the impurity-induced bandgap closing in massive Dirac model. Following Ref. [47], we employ a self-consistent Born approximation that represents the simplest minimal model to take into account impurity/disorder scattering at the homogeneous level. We find that such bandgap closing is not associated with a vanishing of the effective massive term, rather to a diverging of the quasi-particle dynamical renormalization. The role of incoherent processes is also discussed, and the consistency of the present results with Luttinger’s theorem validated.

The paper is organized in three sections. In Section II we give the general formalism of SCBA in Dirac model. In Section III we discuss the effects of the dynamical bandgap renormalization and of the quasiparticle properties. Finally, in Section IV the present results are discussed in relation of possible theoretical scenarios.

II. THE MODEL

In this paper we consider the massive Dirac model described by the Hamiltonian:

$$\hat{H}_{\mathbf{k}} = \hbar v [k_x \hat{\sigma}_x + k_y \hat{\sigma}_y] + \Delta \hat{\sigma}_z, \quad (1)$$

where the term $\propto \hat{\sigma}_z$ induced a gap $\sim 2\Delta$ at the Dirac point $\mathbf{k} = 0$. Mimicking the specific case of graphene, we introduce an upper momentum cut-off k_c chosen to preserve the total available phase space. Namely, considering also the valley degeneracy $N_v = 2$ in graphene, we set $N_v \pi k_c^2 = V_{\text{BZ}}$, where $V_{\text{BZ}} = 8\pi^2/3\sqrt{3}a^2$ is the graphene Brillouin zone and a the nearest-neighbors carbon-carbon distance. Using a typical value $a = 1.42 \text{ \AA}$, we get $k_c = 1.09 \text{ \AA}^{-1}$, which can be associated with an ultraviolet energy cut-off $W = \hbar v k_c = 7.2 \text{ eV}$, so that $\hbar v |\mathbf{k}| \leq W$.

We consider scattering on local impurity centers with density n_{imp} and potential

$$V_{\text{imp}}(\mathbf{r}) = \sum_i V_i \delta(\mathbf{r} - \mathbf{R}_i), \quad (2)$$

where \mathbf{R}_i are the coordinates of the lattice sites. We assume standard Born impurity correlations

$$\langle V_{\text{imp}}(\mathbf{r}) \rangle = 0, \quad (3)$$

$$\langle V_{\text{imp}}(\mathbf{r}) V_{\text{imp}}(\mathbf{r}') \rangle = n_{\text{imp}} V_{\text{imp}}^2 \delta(\mathbf{r} - \mathbf{r}'), \quad (4)$$

where the average $\langle \dots \rangle$ is meant over all the space \mathbf{r} (\mathbf{r}') and over all the impurity configurations. For simplicity we define the parameter $\gamma_{\text{imp}} = n_{\text{imp}} V_{\text{imp}}^2$. With these notations we can write the Born impurity self-energy in the Matsubara space:

$$\hat{\Sigma}(i\omega_n) = \gamma_{\text{imp}} N_v \sum_{\mathbf{k}} \hat{G}(\mathbf{k}, i\omega_n), \quad (5)$$

where the self-consistent Green's function reads:

$$\hat{G}(\mathbf{k}, i\omega_n) = \frac{1}{i\omega_n \hat{I} - \hat{H}_{\mathbf{k}} - \hat{\Sigma}(i\omega_n)}. \quad (6)$$

We can expand the self-energy in Pauli matrices, $\hat{\Sigma} = \Sigma_I \hat{I} + \Sigma_x \hat{\sigma}_x + \Sigma_y \hat{\sigma}_y + \Sigma_z \hat{\sigma}_z$. It is easy to see that the self-energy is momentum-independent and that only the terms $\Sigma_I(i\omega_n)$ and $\Sigma_z(i\omega_n)$ are not zero. The self-energy terms $\Sigma_I(i\omega_n)$, $\Sigma_z(i\omega_n)$ provide a *dynamical* renormalization of the one-particle excitations, $i\tilde{\omega}_n = i\omega_n - \Sigma_I(i\omega_n)$, and of the gap function, $\Delta(i\omega_n) = \Delta + \Sigma_z(i\omega_n)$. It is useful to introduce also the quasi-particle renormalization function $Z(i\omega_n) = 1 - \Sigma_I(i\omega_n)/i\omega_n$.

After few straightforward steps (in Appendix A), we can write the self-consistent relations:

$$\Sigma_I(i\omega_n) = -i\omega_n Z(i\omega_n) U \alpha(i\omega_n), \quad (7)$$

$$\Sigma_z(i\omega_n) = -\Delta(i\omega_n) U \alpha(i\omega_n), \quad (8)$$

where U is the dimensionless parameter, $U = N_v \gamma_{\text{imp}} S_{\text{cell}} / 2\pi \hbar^2 v^2$, and where

$$\alpha(i\omega_n) = \ln \left[1 + \frac{W^2}{\Delta^2(i\omega_n) + \tilde{\omega}_n^2} \right]. \quad (9)$$

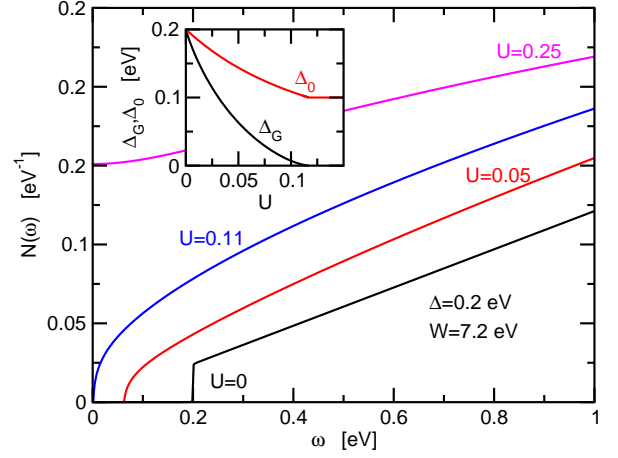


FIG. 1: color online) Density of states $N(\omega)$ for different values of the impurity scattering. We set $\Delta = 0.2 \text{ eV}$ and $W = 7.2 \text{ eV}$. The gap vanishes in the density of states for U above the critical value $U_c \approx 0.117$. Inset: dependence of U of the bandgap edge Δ_G and of the zero-frequency gap function $\Delta_0 = \Delta(\omega = 0)$.

Eqs. (7)-(9) can be easily generalized on the real-frequency axis, $i\omega_n \rightarrow \omega + i\eta$, with $\eta \rightarrow 0$. We get:

$$\Sigma_I(\omega) = -\omega Z(\omega) U \alpha(\omega), \quad (10)$$

$$\Sigma_z(\omega) = -\Delta(\omega) U \alpha(\omega), \quad (11)$$

where $\Delta(\omega) = \Delta + \Sigma_z(\omega)$, $Z(\omega) = 1 - \Sigma_I(\omega)/\omega$, and $\tilde{\omega} = \omega + i\eta - \Sigma_I(\omega)$. All the quantities depending on the real-axis frequency represent here the retarded part, e.g. $\alpha(\omega) = \alpha(\omega + i\eta)$. We have thus explicitly:

$$\alpha(\omega) = \ln \left[1 + \frac{W^2}{\Delta^2(\omega) - \omega^2 Z^2(\omega)} \right]. \quad (12)$$

Once known the self-energy, we can express the spectral function $A(\mathbf{k}, \omega)$ as:

$$\begin{aligned} A(\mathbf{k}, \omega) &= -\frac{1}{\pi} \text{Im} \left\{ \text{Tr} \left[\hat{G}(\mathbf{k}, \omega + i\eta) \right] \right\} \\ &= -\frac{1}{\pi} \text{Im} \left\{ \frac{2\omega Z(\omega)}{\omega^2 Z^2(\omega) - \epsilon_{\mathbf{k}}^2 - \Delta^2(\omega)} \right\}, \end{aligned} \quad (13)$$

and the density of states per spin:

$$N(\omega) = N_v \sum_{\mathbf{k}} A(\mathbf{k}, \omega) = \frac{2}{W^2} \text{Im} [\omega Z(\omega) \alpha(\omega)]. \quad (14)$$

III. BANDGAP RENORMALIZATION

Eqs. (11)-(10) have been introduced in Ref. [47], where also a bandgap closing was predicted, for given U impurity scattering, for values of the bare gap Δ larger than a critical value $\Delta_c(U, W)$. Analytical estimates of $\Delta_c(U, W)$ were provided in the asymptotic limit $U \rightarrow 0$,

but the physics underlying such bandgap closing was not specifically addressed.

The most direct way to trace the evolution of the effective gap as a function of the impurity scattering is the investigation of the renormalized density of state. We *define* thus the bandgap edge Δ_G as the gap observed in the DOS. Some representative cases are shown in Fig. 1, showing how the Δ_G decreases by increasing U until it vanishes above a critical value U_c . The evolution of Δ_G as a function of U can be investigated in a semi-analytical way, as presented in Appendix B, and it is depicted in the inset of Fig. 1. A perturbation analysis can be also derived, predicting in the dilute impurity $U \ll U_c$ the behavior (see Appendix B)

$$\Delta_G \approx \Delta \left\{ 1 - 2U\mathcal{W} \left(\frac{e^4 W^2}{4U\Delta^2} \right) \right\}. \quad (15)$$

where e is the Napier's constant and $\mathcal{W}(z)$ is the Lambert \mathcal{W} -function (or so called ProductLog function) which obeys $\mathcal{W}(z)e^{\mathcal{W}(z)} = z$ and its asymptotic behavior is $\mathcal{W}(z \gg 1) \approx \ln(z) - \ln(\ln(z))$. For the set of parameters used in Fig. 1, this relation results to be accurate only for very low values of U ($U < 0.17U_c \sim 0.02$), pointing out thus the compelling need of a non-perturbative self-consistent analysis.

As discussed in Ref. [47], the critical value U_c above which $\Delta_G = 0$ can be determined by the onset of an imaginary part in the self-energy Σ_I at $\omega = 0$, $\Sigma_I(\omega = 0) = -i\Gamma$ whereas the off-diagonal self-energy, associated with the renormalization of the gap function, $\sigma = -\Sigma_z(\omega = 0)$, remains a purely real quantity. We generalize the analysis of Ref. [47] at any value of U , relaxing the condition $U \ll 1$. The closing of the gap in the density of states is thus ruled by the set of self-consistent equations for Γ and σ :

$$\Gamma = \Gamma U \ln \left[1 + \frac{W^2}{(\Delta - \sigma)^2 + \Gamma^2} \right], \quad (16)$$

$$\sigma = (\Delta - \sigma) U \ln \left[1 + \frac{W^2}{(\Delta - \sigma)^2 + \Gamma^2} \right]. \quad (17)$$

Moreover the density of states at $\omega = 0$ is given by

$$N(0) = \frac{2\Gamma}{W^2} \ln \left[1 + \frac{W^2}{(\Delta - \sigma)^2 + \Gamma^2} \right]. \quad (18)$$

Eqs. (16)-(17) admit thus two possible solutions, for $U \leq U_c$ and for $U \geq U_c$, where

$$U_c = \frac{1}{\ln \left[1 + \frac{4W^2}{\Delta^2} \right]}. \quad (19)$$

For weak impurity scattering $U \leq U_c$ we have thus $\Gamma = 0$ and finite $\sigma \leq \Delta/2$, implying zero density of states $N(0) = 0$, whereas, for $U \geq U_c$, σ gets locked at $\sigma = \Delta/2$

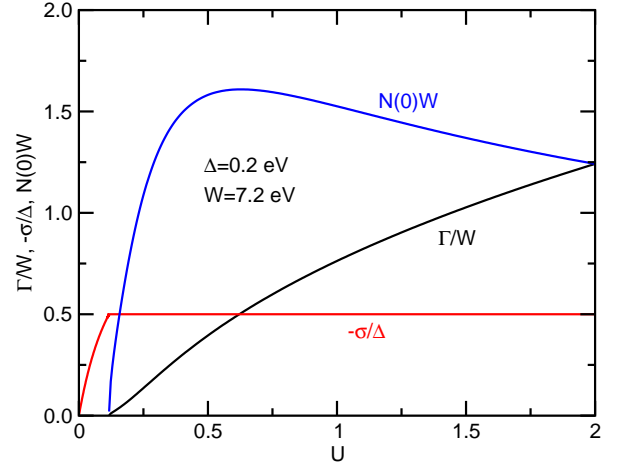


FIG. 2: color online) Dependence on the impurity scattering parameter U of the zero-frequency quantities Γ , σ and $N(0)$. We set $\Delta = 0.2$ eV and $W = 7.2$ eV. For these values we have $U_c = 0.117$.

and Γ finite, with $\Gamma \propto \sqrt{U - U_c}$ for $U \rightarrow U_c^+$. An analytical expression for the density of states at zero energy can be obtained in this regime:

$$N(0) = \frac{2\Gamma(U, \Delta, W)}{UW^2}, \quad (20)$$

where

$$\Gamma = W\Theta(U - U_c) \sqrt{\frac{1}{\exp(1/U) - 1} - \frac{1}{\exp(1/U_c) - 1}}. \quad (21)$$

where $\Theta(x)$ is the Heaviside function. The plot of Γ , σ and $N(0)$ as functions of U is shown in Fig. 2. We also obtain the asymptotic dependences Γ , $N(0) \propto \sqrt{U - U_c}$, for $U \rightarrow U_c^+$, and $\Gamma \propto \sqrt{U}$, $N(0) \propto 1/\sqrt{U}$, for $U \gg U_c$.

The value $\Delta_0 = \Delta(\omega = 0) = \Delta - \sigma$ represents the value of the gap function $\propto \hat{\sigma}_z$ at zero energy excitations, in the presence of disorder/impurity scattering. We note that, as shown in the inset of Fig. 1, unlike Δ_G , Δ_0 is always finite for *any* value of U , signaling that, in the spirit of a renormalization group approach, a finite term $\propto \hat{\sigma}_z$ is always relevant in the low-energy limit $\omega \rightarrow 0$, in agreement with the topological robustness of the massive Dirac model in the presence of a scattering source that does not affect the symmetry properties.

This observation points out that the closing of the bandgap Δ_G cannot be understood in terms of purely *topological* excitations $\propto \hat{\sigma}_z$ associated with $\Delta(\omega)$, but the renormalization of the quasi-particle spectral properties $\propto \hat{\sigma}_I$, associated with $Z(\omega)$, plays a fundamental role.

In order to shed further light on this issue, we analyze the properties of the spectral function, defined in

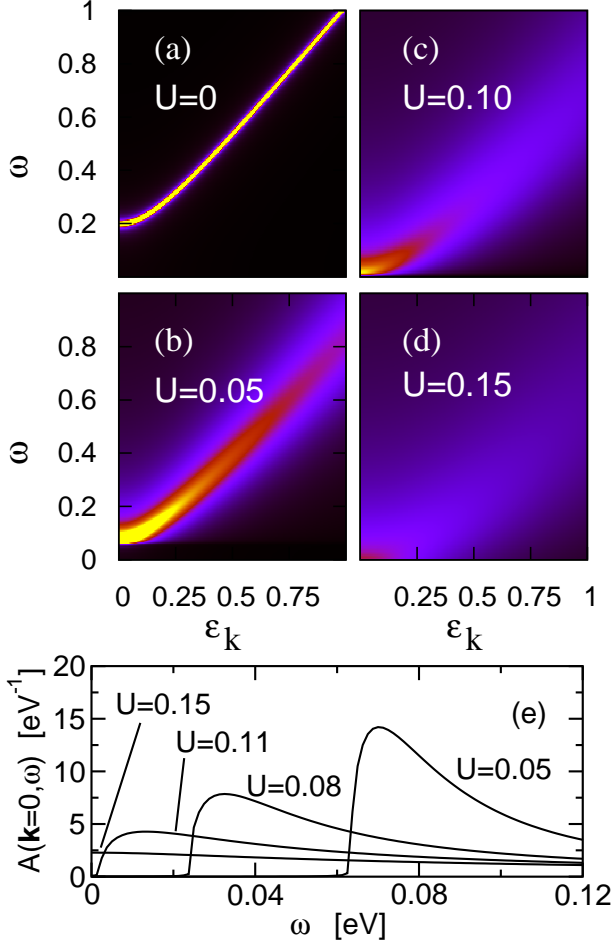


FIG. 3: (color online) (a)-(d) Intensity map of the spectral function $A(\mathbf{k}, \omega)$ for ($U < U_c$) $U = 0$, $U = 0.05$, $U = 0.10$ and ($U > U_c$) $U = 0.15$. Here $\Delta = 0.2$ eV, $W = 7.2$ eV and $\epsilon_{\mathbf{k}} = \hbar v|\mathbf{k}|$. (e) Spectral function $A(\mathbf{k}, \omega)$ at $\epsilon_{\mathbf{k}} = 0$ for $U = 0.05, 0.08, 0.11, 0.15$.

Eq. (13), which can be conveniently rewritten as:

$$A(\mathbf{k}, \omega) = -\frac{2}{\pi} \text{Im} \left\{ \frac{\omega/Z(\omega)}{\omega^2 - [\epsilon_{\mathbf{k}}/Z(\omega)]^2 - \tilde{\Delta}(\omega)^2} \right\}, \quad (22)$$

where $\tilde{\Delta}(\omega) = \Delta(\omega)/Z(\omega)$. The function $Z(\omega)$ is associated with the renormalization of the one-particle spectral weight and of the one-particle dispersion, whereas $\tilde{\Delta}(\omega)$ rules the effective excitations in the presence of the gap and of the dynamical renormalization induced by the scattering processes.

The intensity map of the spectral function $A(\mathbf{k}, \omega)$ for few representative cases in the regimes $U < U_c$ and $U > U_c$ is shown in Fig. 3(a)-(d). A dispersive “quasi-particle” peak in the spectral intensity is detected at low energy for all $U \leq U_c$, whereas any signature of coherent peak disappears for $U \geq U_c$. Note that the “quasi-particle” peak follows the dependence of Δ_G rather than Δ_0 . A similar behavior is traceable in the evolution of

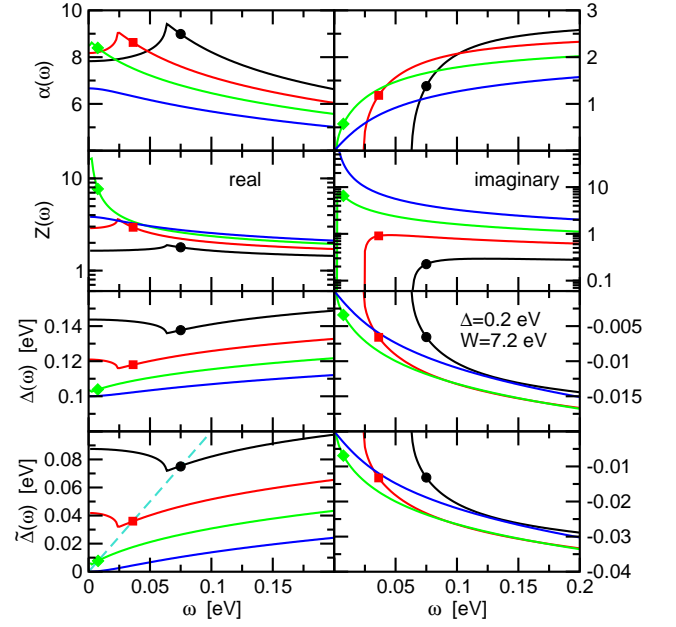


FIG. 4: (color online) Real parts (left panels) and imaginary parts (right panels) of the complex functions $\alpha(\omega)$, $Z(\omega)$, $\Delta(\omega)$, $\tilde{\Delta}(\omega)$, for few representative U : $U = 0.05$ (black), $U = 0.08$ (red), $U = 0.11$ (green), $U = 0.15$ (blue). A coherent gap is determined, for $U \leq U_c$, in the left-bottom panel by the graphical solution of Eq. (23), for $U = 0.05$ (black circle), $U = 0.08$ (red square), and $U = 0.11$ (green diamond). No coherent gap is defined for $U = 0.15 > U_c$. The value of the quantities (real and imaginary parts) for $\omega = \tilde{\Delta}_{\text{coh}}$ in the other panels is also shown by the corresponding symbols.

the spectral function at the bandgap edge $\epsilon_{\mathbf{k}} = 0$, as shown in Fig. 3(e). Most noticeable is here the anomalous (non-Lorentzian) shape of the spectra function, even for $U \leq U_c$ signaling that the coherent quasi-particle picture is questionable and incoherent processes associated with the imaginary parts of the self-energy are here relevant.

To investigate in more detail this issue we plot in Fig. 4 the real (left panels) and imaginary (right panels) parts of the relevant quantities $Z(\omega)$, $\Delta(\omega)$, $\tilde{\Delta}(\omega)$, as well as the function $\alpha(\omega)$.

In the spirit of a picture of quasi-particle coherent excitations, we can *define* a coherent bandgap $\tilde{\Delta}_{\text{coh}}$ at $\epsilon_{\mathbf{k}} = 0$ by *assuming* the imaginary part of the denominator of Eq. (22) to be negligible, and by looking for the zeroes of the real part, i.e.

$$\omega = \text{Re}[\tilde{\Delta}(\omega)] \Big|_{\omega=\tilde{\Delta}_{\text{coh}}}. \quad (23)$$

The value of the coherent bandgap $\tilde{\Delta}_{\text{coh}}$ so obtained, for some relevant values of the impurity scattering, is marked by filled symbols in the left-lower panel, and the values of all the other relevant functions at such energy $\omega = \tilde{\Delta}_{\text{coh}}$ is shown in the other panels.

The resulting dependence of $\tilde{\Delta}_{\text{coh}}$ as a function of

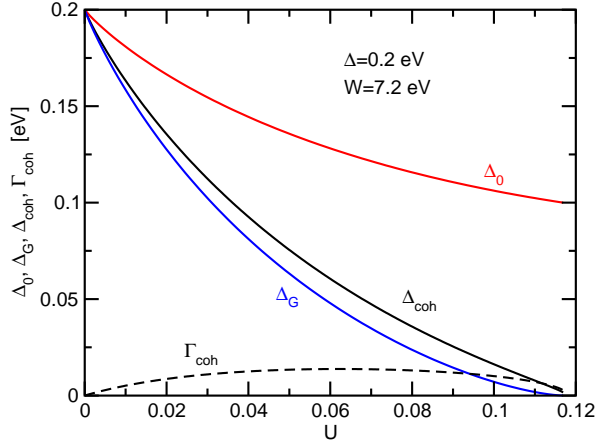


FIG. 5: (color online) Plot of “coherent” bandgap $\tilde{\Delta}_{\text{coh}}$, of the true bandgap Δ_G , of the zero-frequency gap function Δ_0 as function of the dimensionless impurity scattering parameter U . Also shown is the self-consistent damping Γ_{coh} of the coherent bandgap, as defined in Eq. (24).

U , compared with Δ_G and Δ_0 , is shown in Fig. 5. The fair agreement between $\tilde{\Delta}_{\text{coh}}$ and Δ_G shows that, except close to $U \approx U_c$, the gap states can be at a good extent described as quasi-coherent excitations, in accordance with the presence of bright quasi-particle peaks for $U \leq U_c$ in Fig. 3. We can further check the robustness of the coherent-gap approximation, as defined in Eq. (23), by evaluating the expected imaginary part of the gap-function,

$$\Gamma_{\text{coh}} = \text{Im}[\tilde{\Delta}(\omega)] \Big|_{\omega=\tilde{\Delta}_{\text{coh}}}. \quad (24)$$

As expected, $\Gamma_{\text{coh}} \ll \tilde{\Delta}_{\text{coh}}$ for any $U \leq U_c$ (except very close to U_c), supporting the validity of the quasi-coherent gap approximation. On the other hand, although relatively small, a finite imaginary part Γ_{coh} is also always associated with such excitations, giving rise to the asymmetric shape of the spectral function.

Eventually, however, for $U \approx U_c$, the incoherent contribution become dominant, $\Gamma_{\text{coh}} \gg \tilde{\Delta}_{\text{coh}}$, and the effective bandgap closing cannot be described without such incoherent processes.

IV. DISCUSSION AND CONCLUSIONS

In this paper we have investigated, within a self-consistent Born approximation scheme, the effects of disorder/impurity scattering on the one-particle spectral properties of gapped Dirac model. We have shown that the dynamical self-energy leads to a renormalization (reduction) of the bandgap edge. For impurity scattering above a critical value, $U \geq U_c$ the bandgap closes and a finite density of states appears at zero energy. We have shown that such bandgap closing does not stem from a vanishing of the massive term, but it is rather associated

with a divergence of the one-particle dynamical renormalization function. Although a quasi-particle picture can be a good approximation in a wide range of the impurity scattering U , we have shown a finite incoherent weight is always present.

The onset of a finite density of states at zero energy, associated with the closing of the bandgap edge, above a threshold $U \geq U_c$, might appear at odds with the Luttinger’s theorem, according which, in the absence of a phase transition, the area of the Fermi surface (and hence the DOS, for \mathbf{k} -independent self-energies) should be conserved for any value of the scattering interaction. It is however important to underline here that, as we have remarked in the previous Section, a finite imaginary part of the self-energy is strongly tight with the presence of a finite density of states, so that no perfectly coherent excitation with zero damping can be defined, even with zero energy $\omega = 0$. From another point of view, this implies that, technically speaking, a Fermi liquid cannot be defined, questioning thus one of the basic assumptions for the validity of the Luttinger’s theorem. [52, 53] The onset of a finite density of states for $U \geq U_c$, is thus not in contradiction with the Luttinger’s theorem, that cannot be applied here.

Appendix A: Impurity self-energy

We summarize in the present Appendix the details of the derivation of the impurity self-energy in the Born approximation. By using Eqs. (5) and (6), we can immediately write the self-consistent relations for the impurity self-energy in the imaginary-frequency Matsubara space:

$$\Sigma_I(i\omega_n) = -i\tilde{\omega}_n U \int_0^W \frac{2\epsilon d\epsilon}{\tilde{\omega}_n^2 + \epsilon^2 + \Delta(i\omega_n)^2}, \quad (A1)$$

$$\Sigma_z(i\omega_n) = -\Delta(i\omega_n) U \int_0^W \frac{2\epsilon d\epsilon}{\tilde{\omega}_n^2 + \epsilon^2 + \Delta(i\omega_n)^2}, \quad (A2)$$

where $i\tilde{\omega}_n = i\omega_n - \Sigma_I(i\omega_n)$, $\Delta(i\omega_n) = \Delta + \Sigma_z(i\omega_n)$, and where we have introduced a ultraviolet cut-off W for the linear Dirac dispersion $\epsilon = \hbar v k$. Writing $\sum_{\mathbf{k}} = (S_{\text{cell}}/2\pi\hbar^2 v^2) \int d\epsilon \epsilon \int d\theta/2\pi$, we have also defined here the dimensionless parameter $U = N_v \gamma_{\text{imp}} S_{\text{cell}}/2\pi\hbar^2 v^2$. Eqs. (A1)-(A2) can be also written in the more compact form:

$$\begin{aligned} \Sigma_I(i\omega_n) &= -i\tilde{\omega}_n U \alpha(i\omega_n) \\ &= -i\omega_n \frac{U \alpha(i\omega_n)}{1 - U \alpha(i\omega_n)}, \end{aligned} \quad (A3)$$

$$\begin{aligned} \Sigma_z(i\omega_n) &= -\Delta(i\omega_n) U \alpha(i\omega_n) \\ &= -i\Delta \frac{U \alpha(i\omega_n)}{1 + U \alpha(i\omega_n)}, \end{aligned} \quad (A4)$$

where

$$\alpha(i\omega_n) = \int_0^W \frac{2\epsilon d\epsilon}{\tilde{\omega}_n^2 + \epsilon^2 + \Delta(i\omega_n)^2}. \quad (A5)$$

Appendix B: Bandgap edge Δ_G and bandgap closing at U_c

In this Appendix we provide some semi-analytical expressions for the evolution of the bandgap and of the density of states at zero energy $N(0)$ as functions of the impurity scattering.

For a generic impurity scattering parameter U , the density of states is given by Eq. (14) once the complex quantities $Z(\omega)$, $\Delta(\omega)$, $\alpha(\omega)$ are obtained by the self-consistent solution of Eqs. (11-12). A finite density of states $N(\omega)$ at $|\omega| \leq \Delta_G$ is associated with a finite imaginary part of the functions $Z(\omega)$, $\Delta(\omega)$, $\alpha(\omega)$, whereas the gapped region $|\omega| \geq \Delta_G$ is characterized by the existence of a solution of Eqs. (11-12) with purely real quantities $Z(\omega)$, $\Delta(\omega)$, $\alpha(\omega)$.

To evaluate Δ_G , let us assume thus, for given ω , purely real quantities $Z(\omega) = Z_R$, $\Delta(\omega) = \Delta_R$, $\alpha(\omega) = \alpha_R$. They should fulfill the set of equations:

$$\alpha_R = \ln \left[1 + \frac{W^2}{\Delta_R^2 - \omega^2 Z_R^2} \right], \quad (\text{B1})$$

$$\Delta_R = \frac{\Delta}{1 + U\alpha_R}, \quad (\text{B2})$$

$$Z_R = \frac{1}{1 - U\alpha_R}. \quad (\text{B3})$$

Eqs. (B1)-(B3) can be conveniently recast in a more compact form as:

$$A(\alpha_R) = B(\alpha_R), \quad (\text{B4})$$

where

$$A(\alpha_R) = \exp(\alpha_R), \quad (\text{B5})$$

$$B(\alpha_R) = 1 + \frac{W^2(1 + U\alpha_R)^2}{\Delta^2 - \tilde{\omega}_R^2(1 + U\alpha_R)^2}, \quad (\text{B6})$$

and where

$$\tilde{\omega}_R = \omega Z_R. \quad (\text{B7})$$

Eq. (B4), supported with Eqs. (B5)-(B7), can be solved now in a self-consistent way for given $\tilde{\omega}_R$. The graphical solution for different values of $\tilde{\omega}_R$ is shown in Fig. 6a. Real solutions (marked by filled circles) exist for $\tilde{\omega}_R \leq \tilde{\omega}_c$, signaling for these frequencies zero density of states and hence a bandgap, whereas a finite density of states appears for $\tilde{\omega}_R \geq \tilde{\omega}_c$, where no possible real solution of Eqs. (B4)-(B6) exists and a finite imaginary part/density of states is enforced. As clear from Fig. 6a, the critical value ω_c , can be determined by the condition

$$A'(\alpha_R) = B'(\alpha_R), \quad (\text{B8})$$

which, together with Eqs. (B4)-(B7), after few straightforward mathematical steps, provides an analytical implicit expression

$$\tilde{\omega}_c = \sqrt{\Delta_c^2 - \frac{W^2}{\exp(\alpha_c) - 1}}, \quad (\text{B9})$$

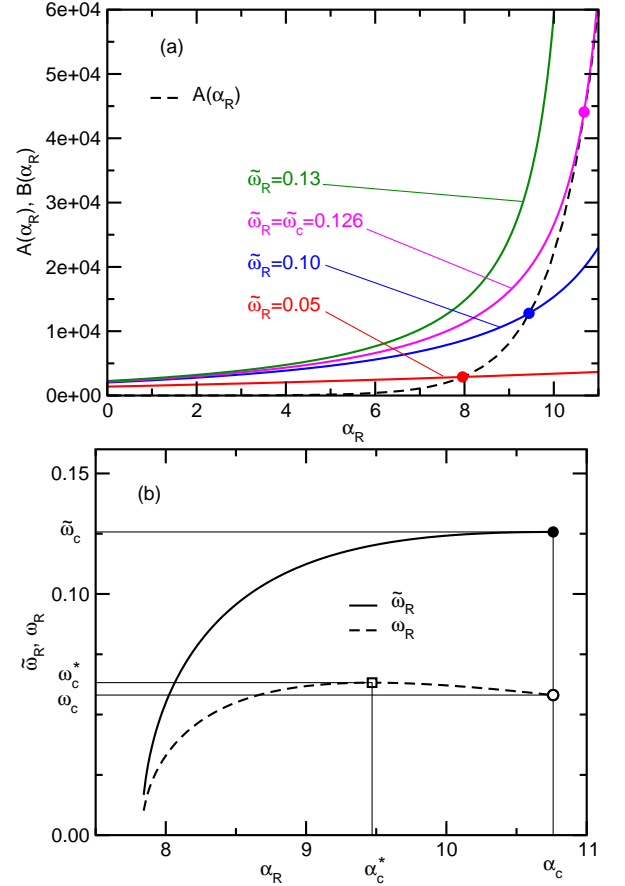


FIG. 6: (color online) (a) Graphical solution of Eq. (B4) for $\Delta = 0.2$ eV and $U = 0.05$. The black dashed line represents the left hand side of Eq. (B4), $A(\alpha_R)$, while the colored solid lines the right hand side $B(\alpha_R)$ for different values of $\tilde{\omega}_R$. A real solution (marked by filled circles) exists for $\tilde{\omega}_R \leq \tilde{\omega}_c$, corresponding to a gapped states. (b) Plot of $\tilde{\omega}_R$ and ω_R vs. α_R . The values α_c , $\tilde{\omega}_c$ and ω_c are marked by empty and filled circles. Note that, due to the non-monotonic behavior, the maximum extension of ω_R , defining the effective bandgap Δ_G , is associated with a value $\omega_c^* > \omega_c$. The value of ω_c^* is marked by a empty square.

where there is a self-consistent relation between Δ_c and α_c :

$$1 = 8U \frac{\Delta_c^3}{\Delta W^2} \sinh^2(\alpha_c/2), \quad (\text{B10})$$

$$\Delta_c = \frac{\Delta}{1 + U\alpha_c}. \quad (\text{B11})$$

Finally, one can write:

$$\omega_c = \tilde{\omega}_c [1 - U\alpha_c]. \quad (\text{B12})$$

The plot of ω_R , $\tilde{\omega}_R$ as functions of α_R for the representative case $\Delta = 0.2$ eV, $U = 0.05$ is shown in Fig. 6b. The filled circle marks here the values of $\tilde{\omega}_c$ and α_c , determining as well to the value of ω_c (empty circle). A important feature to be underlined here, however, is that

there is a monotonic one-to-one dependence between $\tilde{\omega}_R$ and α_R , but no monotonic dependence of ω_R as a function of α_R . The real bandgap edge Δ_G can be thus identified with the largest obtainable value of ω_R which, as evident from Fig. 6b, is not given by ω_c , but rather by $\Delta_G = \omega_c^*$, where ω_c^* can be obtained by the condition $d\omega_R/d\alpha_R = 0$. This condition can be also seen in Fig. 4 where the slope of $\alpha(\omega)$ function diverges when ω approach Δ_G from below.

Such analytical constraint can be enforced by using Eqs. (B4)-(B7). After few technical steps, we can write the implicit relation

$$0 = -2U [1 - U\alpha_c^*] \left[\Delta_*^2 - \frac{W^2}{\exp(\alpha_c^*) - 1} \right] - 2U [1 - U\alpha_c^*]^2 \frac{\Delta_*^3}{\Delta} + [1 - U\alpha_c^*]^2 W^2 \frac{\exp(\alpha_c^*)}{[\exp(\alpha_c^*) - 1]^2}, \quad (\text{B13})$$

where

$$\Delta_* = \frac{\Delta}{1 + U\alpha_c^*}. \quad (\text{B14})$$

In addition, we have

$$\tilde{\omega}_c^* = \sqrt{\Delta_*^2 - \frac{W^2}{\exp(\alpha_c^*) - 1}}, \quad (\text{B15})$$

and

$$\omega_c^* = \tilde{\omega}_c^* [1 - U\alpha_c^*]. \quad (\text{B16})$$

The value ω_c^* in Eq. (B14), along with the self-consistent solution of Eqs. (B13), (B15), (B16), identifies the bandgap $\Delta_G(U) = \omega_c^*$ as a function of the impurity scattering parameter U .

A perturbation approach can be also applied to extract analytically the magnitude of the bandgap reduction in the dilute impurity $U \ll U_c$ regime. After few straightforward steps, we obtain thus:

$$\Delta_G \approx \Delta \left\{ 1 - 2U\mathcal{W} \left(\frac{\mathfrak{e}^4 W^2}{4U\Delta^2} \right) \right\}. \quad (\text{B17})$$

where \mathfrak{e} is the Napier's constant and $\mathcal{W}(z)$ is the Lambert \mathcal{W} -function (or so called ProductLog function) which obeys $\mathcal{W}(z)\mathfrak{e}^{\mathcal{W}(z)} = z$. [54]

The above set of equations (B13)-(B16) can be employed also to investigate the critical value $U = U_c$ at which the bandgap Δ_G closes, i.e. $\Delta_G(U_c) = 0$. Note that, by definition, $\Delta_G = \omega_c^*$ which, as discussed above, does *not* imply $\tilde{\omega}_c^* = 0$. We have thus $\alpha_c^*(U_c) = 1/U_c$, $\Delta_c(U_c) = \Delta/2$ and

$$\alpha_c^*(U_c) = \ln \left[1 + \frac{4W^2}{\Delta^2} \right]. \quad (\text{B18})$$

As a consequence, we can get the final analytical result:

$$U_c = \frac{1}{\ln \left[1 + \frac{4W^2}{\Delta^2} \right]}. \quad (\text{B19})$$

Alternatively, we can look back at Eqs. (B1)-(B2) in the complex space, and consider the case $\omega = 0$. For symmetry we have that $\Sigma_I(\omega = 0) = -i\Gamma$ is a purely imaginary quantity, whereas $\Sigma_z(\omega = 0) = \sigma$ is a purely real one. As a byproduct, also the quantity $\alpha(\omega = 0)$ appears to be a purely real one. We can write a self-consistent set of equations:

$$\Gamma = \Gamma U \ln \left[1 + \frac{W^2}{(\Delta + \sigma)^2 + \Gamma^2} \right], \quad (\text{B20})$$

$$\sigma = -(\Delta + \sigma)U \ln \left[1 + \frac{W^2}{(\Delta + \sigma)^2 + \Gamma^2} \right], \quad (\text{B21})$$

For small U the only possible solution is $\Gamma = 0$. A finite Γ is sustained at a critical value U_c which can be found by the conditions:

$$1 = U_c \ln \left[1 + \frac{W^2}{(\Delta + \sigma)^2} \right], \quad (\text{B22})$$

$$\sigma = -(\Delta + \sigma)U_c \ln \left[1 + \frac{W^2}{(\Delta + \sigma)^2} \right]. \quad (\text{B23})$$

This set of equations imply $\sigma = -\Delta/2$, and an analytical expression for U_c

$$1 = U_c \ln \left[1 + \frac{4W^2}{\Delta^2} \right], \quad (\text{B24})$$

which corresponds to Eq. (B19).

-
- [1] A. H. Castro Neto, F. Guinea, N.M.R. Peres, K.S. Novoselov, and A.K. Geim, *Rev. Mod. Phys.* **81**, 109 (2009).
 - [2] G. W. Semenoff, *Phys. Rev. Lett.* **53**, 2449 (1984).
 - [3] K. S. Novoselov, *Nature Mater.* **6**, 720 (2007).
 - [4] S. Y. Zhou, G.-H. Gweon, A. V. Fedorov, P. N. First, W.

- A. de Heer, D.-H. Lee, F. Guinea, A. H. Castro Neto, and A. Lanzara, *Nature Mater.* **6**, 770 (2007).
- [5] A. Bostwick, T. Ohta, T. Seyller, K. Horn and E. Rotenberg, *Nature Phys.* **3**, 36 (2007).
- [6] A. K. Geim and K. S. Novoselov, *Nature Mater.* **6**, 183 - 191 (2007).

- [7] J. Robertson, *Phys. Rev. B* **29**, 2131 (1984).
- [8] K. Watanabe, T. Taniguchi and H. Kanda, *Nature Mater.* **3**, 404 - 409 (2004).
- [9] F. Amet, J. R. Williams, K. Watanabe, T. Taniguchi, and D. Goldhaber-Gordon, *Phys. Rev. Lett.* **110**, 216601 (2013).
- [10] C. R. Woods, L. Britnell, A. Eckmann, R. S. Ma, J. C. Lu, H. M. Guo, X. Lin, G. L. Yu, Y. Cao, R. V. Gorbachev, A. V. Kretinin, J. Park, L. A Ponomarenko, M. I. Katsnelson, Yu. N. Gornostyrev, K. Watanabe, T. Taniguchi, C. Casiraghi, H. J. Gao, A. K. Geim, and K. S. Novoselov, *Nature Phys.* **10**, 451 (2014).
- [11] M. Yankowitz, J. Xue and B. J. LeRoy, *J. Phys.: Condens. Matter* **26**, 303201 (2014).
- [12] B. Hunt, J. D. Sanchez-Yamagishi, A. F. Young, M. Yankowitz, B. J. LeRoy, K. Watanabe, T. Taniguchi, P. Moon, M. Koshino, P. Jarillo-Herrero, R. C. Ashoori, *Science* **340**, 1427 (2013).
- [13] E. Wang, Xiaobo Lu, S. Ding, W. Yao, M. Yan, G. Wan, K. Deng, S. Wang, G. Chen, L. Ma, J. Jung, A. V. Fedorov, Y. Zhang, G. Zhang and S. Zhou, *Nature Phys.* **12**, 1111 (2016).
- [14] H.-Z. Lu, W.-Y. Shan, W. Yao, Q. Niu, and S.-Q. Shen, *Phys. Rev. B* **81**, 115407 (2010).
- [15] R.-L. Chu, J. Shi, and S.-Q. Shen, *Phys. Rev. B* **84**, 085312 (2011).
- [16] W. Luo and X.-L. Qi, *Phys. Rev. B* **87**, 085431 (2013).
- [17] D. Xiao, G. B. Liu, W. Feng, X. Xu, and W. Yao, *Phys. Rev. Lett.* **108**, 196802 (2012).
- [18] H. Rostami, A. G. Moghaddam, and R. Asgari, *Phys. Rev. B* **88**, 085440 (2013).
- [19] F. D. M. Haldane *Phys. Rev. Lett.* **61**, 2015 (1988).
- [20] C. L. Kane and E. J. Mele *Phys. Rev. Lett.* **95**, 226801 (2005).
- [21] S. Das Sarma, S. Adam, E. H. Hwang, and Enrico Rossi, *Rev. Mod. Phys.* **83**, 407 (2011).
- [22] J. González, F. Guinea, and M. A. H. Vozmediano *Phys. Rev. B* **59**, R2474(R) (1999).
- [23] S. Das Sarma, E. H. Hwang, and W.-K. Tse, *Phys. Rev. B* **75**, 121406(R) (2007).
- [24] A. Bostwick, F. Speck, T. Seyller, K. Horn, M. Polini, R. Asgari, A. H. MacDonald, and E. Rotenberg, *Science* **328**, 999 (2010).
- [25] T. Appelquist, D. Nash, and L. C. R. Wijewardhana, *Phys. Rev. Lett.* **60**, 2575 (1988).
- [26] D. V. Khveshchenko, *Phys. Rev. Lett.* **87**, 246802 (2001).
- [27] D. V. Khveshchenko and H. Leal, *Nucl. Phys. B* **687**, 323 (2004).
- [28] O. Vafek and M. J. Case, *Phys. Rev. B* **77**, 033410 (2008).
- [29] V. Juricic, I. F. Herbut, and G. W. Semenoff, *Phys. Rev. B* **80**, 081405 (2009).
- [30] J. E. Drut and T. A. L  dhe, *Phys. Rev. B* **79**, 165425 (2009).
- [31] G.-Z. Liu, W. Li, and G. Cheng, *Phys. Rev. B* **79**, 205429 (2009).
- [32] O. V. Gamayun, E. V. Gorbar, and V. P. Gusynin, *Phys. Rev. B* **80**, 165429 (2009).
- [33] J. Wang, H. A. Fertig, and G. Murthy, *Phys. Rev. Lett.* **104**, 186401 (2010).
- [34] J. Gonz  lez, *Phys. Rev. B* **82**, 155404 (2010).
- [35] J. Wang, H. A. Fertig, G. Murthy, and L. Brey, *Phys. Rev. B* **83**, 035404 (2011).
- [36] V. N. Kotov, B. Uchoa, V. M. Pereira, A. H. Castro Neto, and F. Guinea, *Rev. Mod. Phys.* **84**, 1067 (2012).
- [37] J. Gonz  lez, *Phys. Rev. B* **85**, 085420 (2012).
- [38] J. Gonz  lez, *JHEP* **08**, 27 (2012).
- [39] J.-R. Wang and G.-Z. Liu, *New J. Phys.* **14**, 043036 (2012).
- [40] C. Popovici, C. S. Fischer, and L. von Smekal, *Phys. Rev. B* **88**, 205429 (2013).
- [41] E. Cappelluti, L. Benfatto, M. Papagno, D. Pacil  , P. M. Sheverdyaeva, and P. Moras, *Ann. Phys. (Berlin)* **526**, 387 (2014).
- [42] V. M. Pereira, F. Guinea, J. M. B. Lopes dos Santos, N. M. R. Peres, and A. H. Castro Neto, *Phys. Rev. Lett.* **96**, 036801 (2006).
- [43] N. M. R. Peres, F. Guinea, and A. H. Castro Neto, *Phys. Rev. B* **73**, 125411 (2006).
- [44] V. M. Pereira, J. M. B. Lopes dos Santos, and A. H. Castro Neto, *Phys. Rev. B* **77**, 115109 (2008).
- [45] B. D  ra, K. Ziegler, and P. Thalmeier, *Phys. Rev. B* **77**, 115422 (2008).
- [46] B. Yu-Kuang Hu, E. H. Hwang, and S. Das Sarma, *Phys. Rev. B* **78**, 165411 (2008).
- [47] Y. Arimura and T. Ando, *Journal of the Physical Society of Japan* **81**, 024702 (2012).
- [48] J. W. Gonz  lez and J. Fern  ndez-Rossier *Phys. Rev. B* **86**, 115327 (2012).
- [49] A. V. Balatsky, I. Vekhter, and Jian-Xin Zhu, *Rev. Mod. Phys.* **78**, 373 (2006).
- [50] T. O. Wehling, A.M. Black-Schaffer, and A.V. Balatsky, *Advances in Physics*, **63**, 76, (2014).
- [51] Eduardo V. Castro, M. Pilar L  pez-Sancho, and Mar  a A. H. Vozmediano *Phys. Rev. B* **92**, 085410 (2015).
- [52] J. M. Luttinger and J. C. Ward, *Phys. Rev.* **118**, 1417 (1960).
- [53] J. M. Luttinger, *Phys. Rev.* **119**, 1153 (1960).
- [54] See the following link for more information about Lambert W-function: mathworld.wolfram.com